Design, fabrication, and performance of spin-valve read heads for magnetic recording applications

by C. H. Tsang R. E. Fontana, Jr. T. Lin D. E. Heim

B. A. Gurney M. L. Williams

Since the early 1990s, the introduction of dualelement recording heads with inductive write elements and magnetoresistive (MR) read elements has almost doubled the rate of areal density improvements for hard-disk-drive data storage products. In the past several years, prospects of even more rapid performance improvements have been made possible by the discovery and development of sensors based on the giant magnetoresistance (GMR) effect, also known as the spin-valve effect, for a particular class of sensor configurations. In this paper, we explore the potentials as well as challenges of spin-valve sensors as magnetic recording read heads. We first examine the data rate and areal density potentials of large

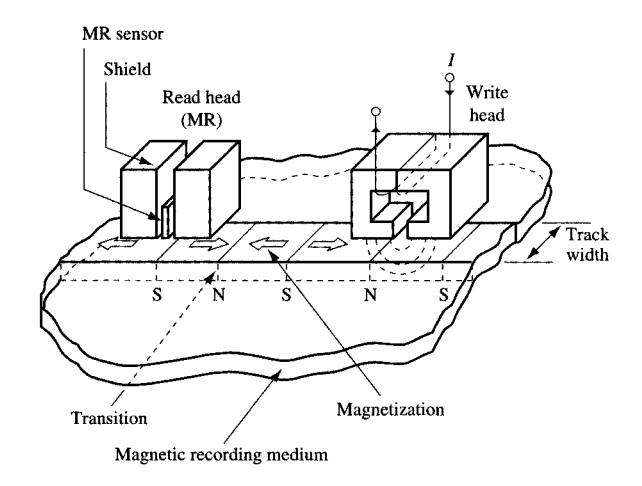
read-back signals resulting from increases in the MR coefficient. We then discuss associated magnetic sensor performance, including linearity and noise suppression. Finally, we study in detail the magnetic and recording performance of a spin-valve read head designed for 1-Gb/in.² density performance.

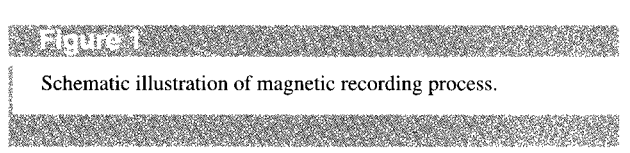
Introduction

Magnetic recording systems which utilize magnetic disk and tape drives constitute the main form of data storage and retrieval in present-day computer and data processing systems. The principles of magnetic recording are illustrated schematically in **Figure 1**. In the recording

Copyright 1998 by International Business Machines Corporation. Copying in printed form for private use is permitted without payment of royalty provided that (1) each reproduction is done without alteration and (2) the *Journal* reference and IBM copyright notice are included on the first page. The title and abstract, but no other portions, of this paper may be copied or distributed royalty free without further permission by computer-based and other information-service systems. Permission to *republish* any other portion of this paper must be obtained from the Editor.

0018-8646/98/\$5.00 © 1998 IBM





process, information is written and stored as magnetization patterns on the magnetic recording medium. This is done by scanning the write head over the medium and energizing the write head, which is basically an electromagnet, with appropriate current waveforms. Next, in the read-back process, the stored information is retrieved by scanning a read head over the recording medium. The read head intercepts magnetic flux from the magnetization patterns on the recording medium and converts it into electrical signals which are then detected and decoded. A very important performance criterion for a disk recording system is the amount of information it can store per unit area. Since information is typically stored as abrupt magnetization changes, designated as transitions, along a track on the disk (Figure 1), the areal density is the product of the linear bit density and the track density. The former is the density with which magnetic transitions can be packed along a track; the latter is the density with which these tracks can in turn be packed together. A high track density therefore implies recording with narrow tracks. The areal density performance of disk recording systems has increased consistently and dramatically for the last thirty years, culminating in an improvement by more than five orders of magnitude from 2 Kb/in.² for the first disk drive (the RAMAC*) introduced by IBM in the late 1950s to more than 1 Gb/in.² for the company's 1996 DASD products. Such rapid and sustained progress has been made possible by a continuous series of improvements and revolutions in disks and especially heads.

Traditionally, the recording head is a single inductive element energized as an electromagnet for writing and used according to Faraday's effect for reading. Early inductive heads were made primarily from individually machined polycrystalline ferrites (e.g., MnZn ferrite) wound with fine wires as write and read coils. As areal density increased, the requirements of narrower track geometries and higher write fields led in the late 1970s and early 1980s to the development of metal-in-gap (MIG) ferrite heads for higher write fields, and thin-film inductive heads using photolithographic techniques for narrow track definition and mass production as well as higher write fields. In the early 1990s, after decades of research and development, dual-element heads with inductive write elements and magnetoresistive (MR) read elements were successfully introduced into IBM's DASD products. In these dual-element heads, writing is performed by energizing the inductive element as an electromagnet as before, but reading is performed by the interception of magnetic flux by a magnetoresistive sensor [1]. This leads to a modulation of the sensor resistance through the magnetoresistance effect, which is in turn converted into voltage signals by passing a sense current through the sensor. In comparison with the single inductive recording heads, the dual-element heads have the advantages of separate optimization of read and write performance, as well as a signal sensitivity which is several times larger because of the use of MR sensors. These improvements have led to even more rapid advances in recording areal density [2-5], as exemplified by the recent publication of a 5-Gb/in.² recording demonstration [5] by IBM using dualelement heads, low-noise thin-film disks, and PRML channels.

Since the early 1990s, the limits of MR sensor performance have been drastically expanded by the discovery of the giant magnetoresistance (GMR) effect [6-20], also known as the spin-valve effect [7], for a particular class of sensor configurations. In contrast to the conventional MR effect, which is based on anisotropic magnetoresistance (AMR) present in homogeneous ferromagnetic metals or alloys, the GMR effect is present only in heterogeneous magnetic systems with two or more ferromagnetic components and at least one nonmagnetic component. The spin-dependent scattering of current carriers by the ferromagnetic components results in a modulation of the total resistance by the angles between the magnetizations of the ferromagnetic components. An example is the trilayer permalloy/copper/permalloy system [7], where the GMR effect operates to produce a minimum resistance for parallel alignment of the permalloy magnetizations, and a maximum resistance for antiparallel alignment of the permalloy magnetizations. The first and most attractive feature of the GMR effect for recording head applications is a large increase in the available sensor output, made possible by the large magnitude of the GMR coefficient. The GMR coefficient

104

for a multilayer system is defined as the fractional resistance change between parallel and antiparallel alignment of the adjacent layers. This coefficient can be as high as $\sim 10\%$ [7] for trilayer systems and more than 20% [8] for multilayer systems, in comparison with conventional MR coefficients of only 2-4%. Additionally, the GMR systems are usually optimal at very small magnetic layer thicknesses (~50 Å), resulting in enhancements of magnetic sensitivity from flux concentration effects. Also, in contrast to the quadratic nature of the conventional MR effect, the GMR effect is intrinsically linear in a spin-valve sensor configuration. This in principle should simplify sensor designs in the area of transverse biasing considerations. Finally, in the GMR sensors, the direction of the sense current is unimportant to the operation of the GMR effect. This new feature gives the GMR sensors additional design flexibilities and options. There are, however, also serious technical challenges in applying the GMR sensors to the recording environment. First, most of the high-GMR-coefficient systems have to date exhibited low permeabilities because of strong coupling between the magnetic layers. Until this coupling is significantly reduced, these systems would not be attractive for head applications despite the large size of the GMR coefficients. Second, the magnitude of the GMR effect depends critically on the thicknesses of the thin (<100 Å) magnetic layers and the even thinner (<30 Å) spacer layers. This dependence escalates the quality control requirements of thin-film deposition processes to an unprecedented level. The thinness of the multilayer components also renders the GMR system especially vulnerable to thermal degradation effects caused by interdiffusion, as well as chemical and electrical damage during fabrication and testing. Finally, since the output of a GMR sensor depends on the relative magnetic orientations of two or more very thin magnetic layers, the resultant device behavior could quickly become very complicated compared with that for AMR sensors. This could create new issues in linearization and magnetic noise suppression.

In this paper, using the spin-valve sensor configuration as our reference, we explore its potentials as well as challenges as magnetic recording read heads. We first examine the data rate and areal density potentials of large readback signals due to increases in the MR coefficient. We then discuss the associated magnetic sensor performance, including linearity and noise suppression. Finally, we study in detail the magnetic and recording performance of a spin-valve read head designed for 1-Gb/in.² density performance [15].

Data rate and areal density potentials

The main advantage of a spin-valve sensor over an AMR sensor is that a significant increase occurs in signal output

because of the larger magnitude of typical spin-valve coefficients compared to AMR coefficients. To explore the effects of such a signal increase in extending data rate and areal density performance, we consider the recording system in the published 3-Gb/in.² recording demonstration as our reference [4]. In the reference recording demonstration, an AMR read head with a 120-Å-thick permalloy MR layer was used. In addition, the sensor had a read track width of 1.1 μ m, a stripe height of 0.5 μ m, and a total read gap of 0.20 µm. The resultant read head exhibited a total sheet resistance of 17 Ω/\Box and an MR coefficient of 1.8%. In recording tests on a medium of 0.60 memu/cm² in areal moment, a read-back sensitivity of \sim 520 μ V/ μ m was achieved with a sense current corresponding to a temperature increase from ambience of about 30°C. Using a PRML channel at low on-track error rates (10⁻¹⁰) and reasonable off-track tolerance, the linear density of 180 Kbpi and the track density of 16.7 Ktpi were achieved, corresponding to an areal density of 3 Gb/in.² at a data rate of 5 MB/s. In the present study, we assume that the AMR sensor is replaced by a spin-valve sensor, resulting in an increased MR coefficient in the range of 2-8%, but having a similar sheet resistance. To analyze the data rate and data density impacts of such a change, we use the peak jitter performance projection algorithm described in a previous work [3]. In this algorithm, lowerror-rate performance can be projected from high values of a figure of merit (F) given by

$$F = \frac{TW}{j_{\rm T}},\tag{1a}$$

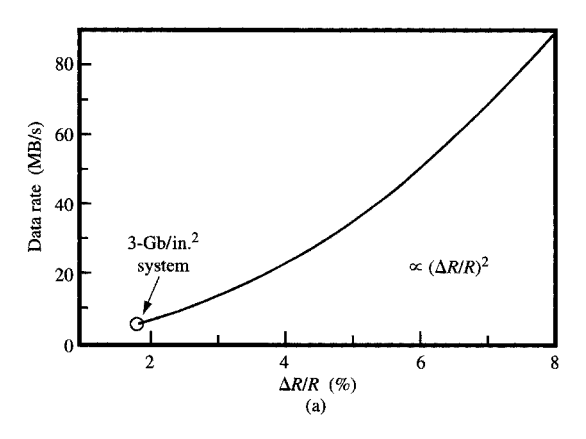
where TW is the "timing" window assuming peak detection and is inversely proportional to the linear density of operation, while $j_{\rm T}$ is the total peak jitter of the read-back waveform. For our reference system, TW is 46.2 nm, $j_{\rm T}$ is 7.3 nm, and F is about 6.3 for 10^{-10} on-track error. The total jitter $(j_{\rm T})$ is composed of jitter from head and electronics noise $(j_{\rm c})$ and jitter from disk noise $(j_{\rm d})$, as follows:

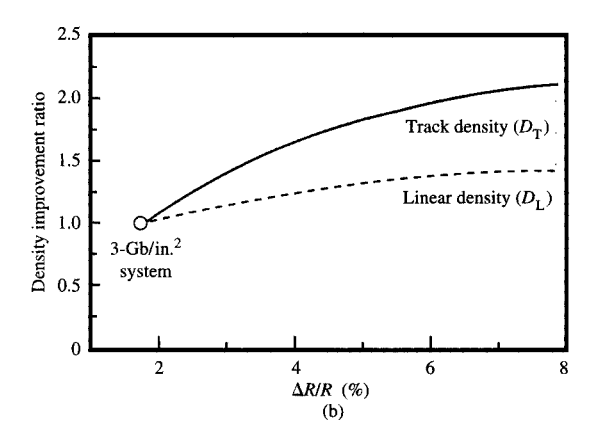
$$j_{\rm T} = \sqrt{j_{\rm e}^2 + j_{\rm d}^2}$$
 (1b)

To study the impact of the MR coefficient on recording performance, we need to know its effects on both types of peak jitter. Assuming the active parameters to be the MR coefficient (s), linear density ($D_{\rm L}$), track density ($D_{\rm T}$), and data rate (r) only, we can simplify the expression for the head and electronics noise jitter to

$$j_{\rm c} = \alpha \frac{D_{\rm L} D_{\rm T} \sqrt{r}}{s},\tag{2a}$$

where s, $D_{\rm L}$, $D_{\rm T}$, and r are normalized relative to our reference 3-Gb/in.² system. Next, the expression for the





Floring 2

(a) Projection of data rate performance vs. GMR coefficient; (b) projection of linear and track density performance vs. GMR coefficient.

disk noise jitter is relatively simple, since it depends upon only the track density,

$$j_{\rm d} = \beta \sqrt{D_{\rm T}} \,. \tag{2b}$$

Finally, the timing window can be expressed in terms of the linear density as

$$TW = \gamma \frac{1}{D_{I}}.$$
 (2c)

Using Equation (1b) and Equations (2), we can rewrite Equation (1a) as

$$\alpha^2 \frac{D_{\rm L}^2 D_{\rm T}^2 r}{s^2} + \beta^2 D_{\rm T} = \frac{\gamma^2}{D_{\rm L}^2 F^2}.$$
 (3)

This equation expresses the relationship among the MR coefficient, data rate, and data densities at a given figure of merit F for recording performance. We are now ready to investigate the exploitation of MR coefficient increases for data rate and data density improvements.

First, to investigate data rate improvements, we assume that the linear and track densities are constant and thus set $D_{\rm I}$ and $D_{\rm T}$ to unity. We obtain

$$s = \frac{\alpha \sqrt{r}}{\sqrt{\left(\frac{\gamma}{F}\right)^2 - \beta^2}},\tag{4a}$$

in which the data rate (r) increases rapidly as the square of the MR coefficient. This dependence is plotted in **Figure 2(a)**, showing a rapid increase in data rate from the reference value of 5 MB/s to beyond 50 MB/s for an MR coefficient of 6% or higher. Clearly, the increase of MR coefficients from spin-valve sensors should be very

effective in extending recording performance toward high-data-rate regimes. We should note, however, that in focusing our analysis on the impacts of the MR coefficient, our model has considered only read-back signal-to-noise performance. In practice, for high-data-rate operations, the degradation of the write head performance due to eddy current and inductance effects, the limitations of the read/write electronics, and the availability as well as the noise performance of the data detection channel will constitute important or even dominant issues over read-back signal-to-noise performance, and will require solutions beyond the improvement of the read head achieved by using a spin-valve rather than an AMR sensor.

Next, to investigate track density improvements we set the data rate and linear density to unity, obtaining

$$s = \frac{\alpha D_{\rm T}}{\sqrt{\left(\frac{\gamma}{F}\right)^2 - \beta^2 D_{\rm T}}}.$$
 (4b)

We observe that the track density varies sublinearly with the MR coefficient because of the increasing importance of disk noise effects (β) as the track widths become narrower. In fact, the improvement reaches an asymptotic ratio of $D_T \approx (\gamma/\beta F)^2$ that cannot be exceeded regardless of the size of the MR coefficient. The resultant behavior can be plotted as in Figure 2(b), which shows an asymptotic track density improvement ratio of about 2 from the reference 3-Gb/in.² system. As a result, track density improvements of almost a factor of 2 should be possible for MR coefficients of 6% or more. Clearly, increases in MR coefficients should also be very helpful in improving track densities, although not as dramatically as

106

in improving data rates. Also, as the track density is increased, narrow-track writing, side-track reading, and head-to-track misregistrations should be important or might even become dominant over read-back signal-to-noise performance in limiting the actual track densities of a recording system.

Finally, to investigate linear density improvements we set data rate and track density to unity, obtaining

$$s = \frac{\alpha D_{\rm L}^2}{\sqrt{\left(\frac{\gamma}{F}\right)^2 - \beta^2 D_{\rm L}^2}}.$$
 (4c)

We observe that the linear density varies less rapidly than the square root of the MR coefficient because of the combined effects of increasing noise effects and reducing timing windows as the linear density of operation becomes higher. Also, the improvement reaches an asymptotic ratio of $D_1 \approx \gamma/\beta F$ that cannot be exceeded regardless of the size of the MR coefficient. This asymptotic ratio is the square root of that for track density improvements, so that distinctly less potential improvement is available for linear density. The resultant behavior is also plotted in Figure 2(b), showing an asymptotic linear density improvement ratio of about 1.5 from the reference 3-Gb/in.² system. As a result, track density improvements of about 1.4 should be possible for MR coefficients of 6% or more. Therefore, increases in the MR coefficient should also be quite helpful in improving linear densities, although comparatively, the increases might be much more efficiently exploited for data rate or track density improvements. In summary, data rate improvement should be the most effective exploitation of the large MR coefficient associated with the use of spin-valve sensors, followed by track density and, finally, linear density improvements. In practice, in an optimal recording system, increases in the MR coefficient are likely to be exploited for a combination of both data rate and data density improvements that can effectively complement the strengths and limitations of other recording components.

Linearization of spin-valve sensor response

To discuss the issue of linearization, we consider the spinvalve sensor configuration [7, 14, 15] shown schematically in **Figure 3**. It consists of a ferromagnetic free layer and a ferromagnetic reference layer separated from each other by a thin spacer layer. The magnetic moment M_2 of the reference layer is pinned along the transverse direction, typically by exchange coupling with an antiferromagnetic layer (e.g., FeMn), while the magnetic moment M_1 of the free layer is allowed to rotate in response to signal fields. The resultant spin-valve response is given by

$$\Delta R \propto \cos(\theta_1 - \theta_2) \propto \sin \theta_1 \,, \tag{5}$$

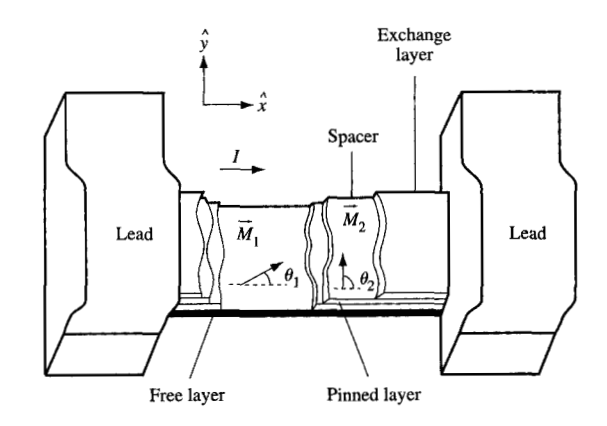
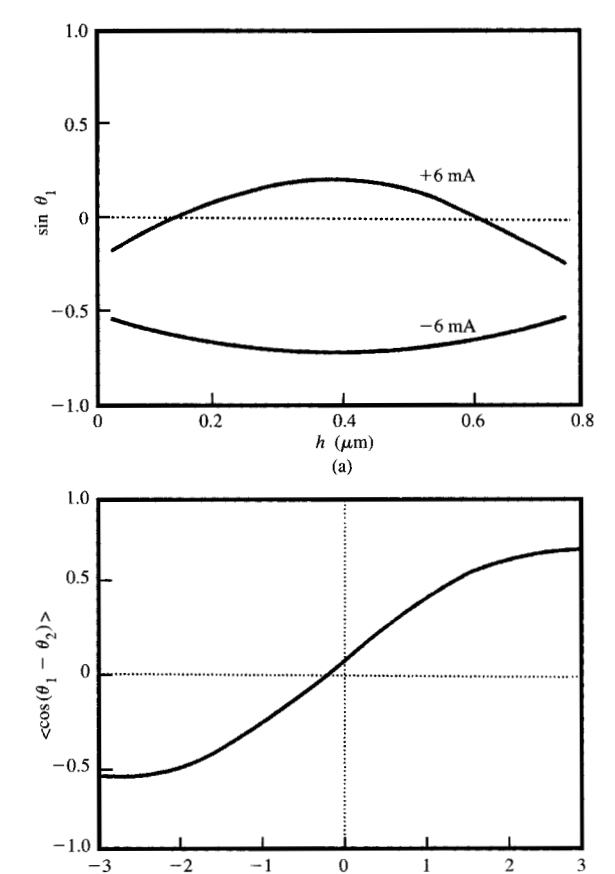


Figure 3

Schematic illustration of a spin-valve sensor.

where θ_1 and θ_2 (= $\pi/2$) represent the directions of freeand pinned-layer magnetic moments, respectively (Figure 3). If the uniaxial anisotropy hard axis of the free layer is oriented along the transverse signal field direction, the magnetic signal response is linear (sin $\theta_1 \propto H$), yielding in turn a linear spin-valve sensor response through Equation (5). This linear spin-valve sensor response is in contrast to the parabolic signal response of conventional AMR sensors [2, 5]. We note, however, that the linearity of the spin-valve response depends first on the precise transverse magnetic orientation of the reference layer and second on the linearity of the magnetic behavior of the free layer in the transverse direction. If the pinning field of the reference layer is not high enough compared with the transverse demagnetization field, the reference layer will become nonuniformly demagnetized from the transverse direction near the upper and lower edges of the sensor. Also, if the exchange-bias pinning field is misaligned from the transverse direction, the magnetization of the reference layer will be canted as a whole from the transverse direction. In both cases, the θ_2 terms in Equation (5) will not be $\pi/2$, resulting in a nonlinear spinvalve response. In addition, if the uniaxial anisotropy easy axis of the free layer were canted from the longitudinal direction or if the free layer were under the influence of a strong longitudinal bias direction, the magnetic response $(\sin \theta_1)$ of the free layer would no longer be linear with the external magnetic field, resulting also in nonlinearities in the spin-valve response. Finally, the spin-valve sensor typically incorporates free layers that also exhibit AMR responses, although the net AMR response might be rather weak because of the thinness of the free layer and the shunting of the other layers. If the AMR response is not completely negligible compared with the spin-valve



Theoretical bias profile (a) and transfer curve (b) for optimized sensor design.

Excitation from medium (normalized)

(b)

response, the resultant sensor response is modified from the simple linear spin-valve response by the presence of a parabolic nonlinearity from residual AMR response. This discussion shows that the maintenance of a linear spin-valve response characteristic is an important task requiring proper operation of various components of the spin-valve sensor.

We now assume that a linear spin-valve response characteristic has indeed been established to allow linear detection of magnetic signals about the quiescent state. The linear operation of the spin-valve sensor terminates when the free-layer magnetic moment becomes saturated along either the up or the down transverse direction. To maximize the signal range capability, it is therefore important to design the spin-valve sensor with the magnetic moment of the free layer oriented along the "unbiased" longitudinal direction in the quiescent state

[14]. This magnetic arrangement constitutes optimal biasing for the spin-valve sensor, which is very different from optimal biasing for an AMR sensor, where the magnetic moment of the AMR layer would be canted at ~45° from the longitudinal direction. The achievement of a longitudinal alignment for the free layer is, however, in practice every bit as challenging as achieving a 45° alignment for a conventional AMR sensor. The reason is that for a small sensor such as that used in the read head, at least three forces are at work to induce transverse orientation of the free layer. First, the magnetostatic coupling between the free layer and the pinned layer along the upper and lower edges of the sensor is usually very substantial for micron-size sensor geometries. This coupling favors antiparallel alignment of the two layers, and its magnitude depends mainly on the thicknesses and the height of the sensor, as well as the presence of shields around the sensor. It also varies quite nonuniformly along the height of a shielded sensor, being strongest near the center and falling off toward the edges. Second, because of the thinness of the conductive spacing between the free layer and the reference layer, a ferromagnetic interlayer coupling is usually also present, brought about presumably by magnetostatic coupling across ripples as slight departures from perfect flatness in the two layers. This ferromagnetic coupling favors parallel alignment, and its magnitude depends upon variables such as substrate flatness and film morphologies, which are quite difficult to measure or control precisely. Third, the application of a sense current in the spin-valve device typically creates a significant transverse bias field. This current-induced bias field may favor parallel or antiparallel alignment depending on the current polarity, and its magnitude depends on both the sense current and the sensor stripe height. The final magnetic state of the free layer depends on the sum of the magnetostatic edge coupling, the ferromagnetic coupling, and the current bias field. For an optimal spin-valve design, the sum of the three effects must be close to zero to allow a net longitudinal orientation of the free layer. For small sensors, since the magnetostatic effect is the strongest of the three effects, the sense-current polarity is typically chosen to result in an addition of the current bias effect and the ferromagnetic coupling to counterbalance the magnetostatic effects. Furthermore, since the three effects in general exhibit quite different dependencies on sensor parameters, the optimal biasing arrangement set up for a given sensor configuration may be disrupted if one or more sensor parameters is altered.

The rather complicated magnetic situation in spin-valve sensor biasing is best studied by a detailed micromagnetic model [14, 15]. Such a model uses as its inputs the resistivities, anisotropies, coupling fields, and thicknesses of the pinned and the free magnetic layers as well as the

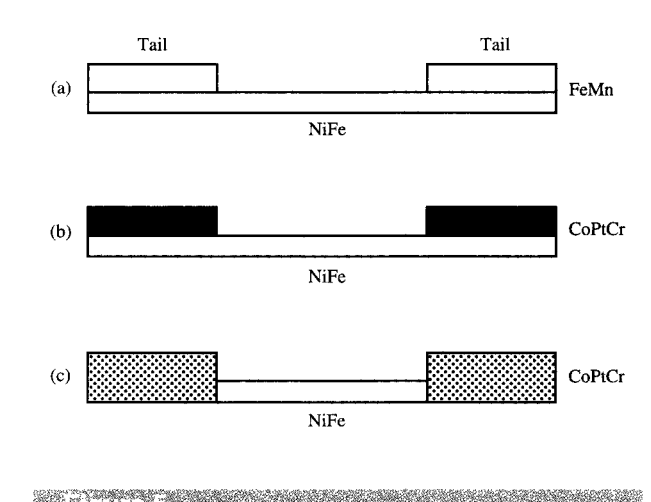
C. H. TSANG ET AL.

height of the sensor. It then employs a finite-element algorithm to determine the biasing profile and the transfer curve response to magnetic flux excitations, as from transitions in recording. Results indeed show that longitudinal alignment of the free layer can be achieved when antiparallel tendencies from the magnetostatic edge coupling are on the average canceled by parallel tendencies from the sum of the interlaver coupling and the sense-current biasing effect. Figure 4(a) shows the magnetic bias profile of the free layer for such an optimized spin-valve sensor design [15] (50 Å Ta/100 Å NiFe/25 Å Cu/22 Å Co/110 Å FeMn). For a positive sense current of 6 mA, the free-layer magnetic moment is seen to be roughly longitudinal ($\theta_1 \sim 0$). The nonuniformity of the magnetostatic coupling effect, however, precludes its perfect cancellation by the ferromagnetic coupling and the current-biasing effects, so that the free-layer magnetic moment actually varies by up to $\pm 20^{\circ}$ about the longitudinal direction along the height of the sensor. Figure 4(b) shows the theoretical transfer curve of the optimized design, with a linear response region terminated at both ends by magnetic saturation effects. The quiescent state of the sensor is around the middle of the linear response region, yielding a maximum signal dynamic range for linear operation.

Magnetic stabilization of spin-valve sensors

The magnetic stabilization of AMR sensors has been an important subject for research and development in the past twenty years [21-26] because small-geometry MR sensors exhibit a spontaneous tendency to break up into complicated multidomain states, leading to serious Barkhausen noise problems during sensor operations. Past studies [23] had shown that, among many factors, the shape demagnetization effect is the primary cause for multidomain formation. This understanding has led to the development of tail stabilization [24] (Figure 5), in which the read region of the sensor is stabilized in a singledomain state by preparing longitudinally aligned tail regions on both sides of the read region. The longitudinally aligned tail regions can be created by exchange-biasing of a soft-magnetic layer with either an antiferromagnet [Figure 5(a): NiFe/FeMn] or a hard ferromagnet [Figure 5(b): NiFe/CoPtCr]. It can also be created by using a longitudinally aligned hard-magnet layer [Figure 5(c): CoPtCr] as the only magnetic layer in the tail region [26]. For narrow-track-width geometries, the longitudinal magnetostatic field created by the aligned tail regions is usually strong enough to induce a singledomain state in the read region.

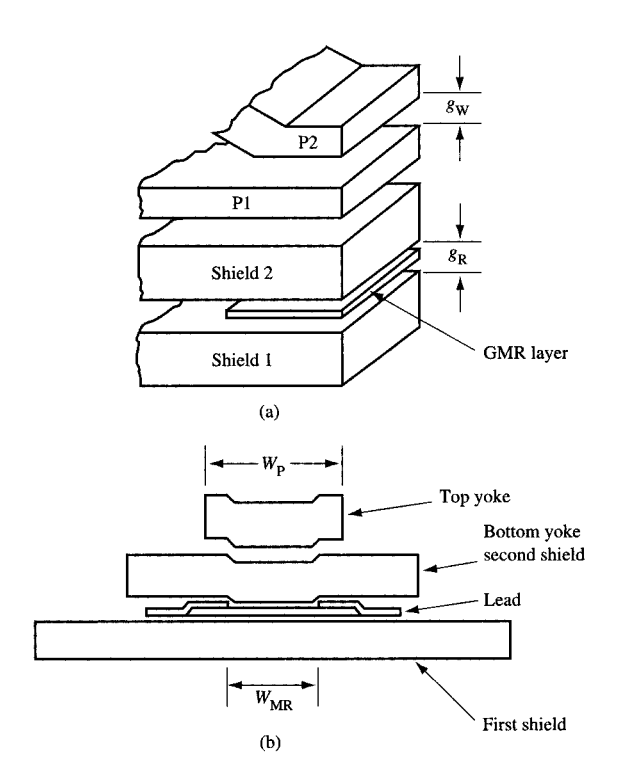
The magnetic stabilization of spin-valve sensors is conceptually similar to that of AMR sensors, so that the various tail-stabilization approaches should also apply in principle. There are however, several differences in detail. First, in the spin-valve sensor, there is only one magnetic



Schematic illustration of means to achieve tail stabilization: (a)

Exchange bias; (b) hard-magnet bias; (c) pure hard-magnet tail.

layer that needs stabilization: the free layer. The reference layer is already well pinned in the transverse direction for proper spin-valve operation and so should not constitute a concern for magnetic stability. This represents a considerably simpler situation than typical soft-adjacentlayer-biased AMR sensors, for which both the MR layer and the soft adjacent layer need stabilization. Second, the thickness of the spin-valve free layer is typically much less than that of an AMR sensor. As a result, the tailregion stabilization layer is also much thinner and therefore more difficult to control precisely to obtain the appropriate tail-to-read-region moment ratio. Third, the stabilized spin-valve sensor typically comprises two pinned layers set along orthogonal directions: the read-region reference layer in the transverse direction and the tailregion magnetic layer in the longitudinal direction. This creates the issue of how to separately orient these two layers without mutual interference. Since the read-region reference layer is typically pinned by exchange-bias with an antiferromagnet [25] (e.g., FeMn, IrMn), it can be oriented by first heating the sensor to beyond the blocking temperature of the antiferromagnet and then cooling the sensor in a transverse aligning field. If the tail region is also pinned by exchange-bias with an antiferromagnet, the tail-region antiferromagnet must have, for example, a distinctly higher blocking temperature than the readregion antiferromagnet. This allows longitudinal orientation of the tail region at a high temperature, to be followed by transverse orientation of the read region at a lower temperature. This requirement of a distinctly higher blocking temperature severely limits the choice and availability of antiferromagnets for the tail regions. To



Schematic illustration of a dual-element GMR head: (a) Stereo view; (b) air-bearing surface view showing shared bottom voke/second shield.

avoid such blocking-temperature conflicts, the tail region could be stabilized instead by the use of hard magnets.

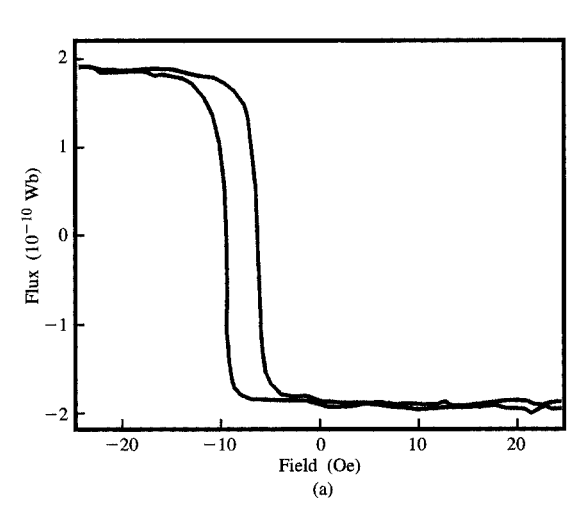
Study of a spin-valve read head for 1-Gb/in.² applications

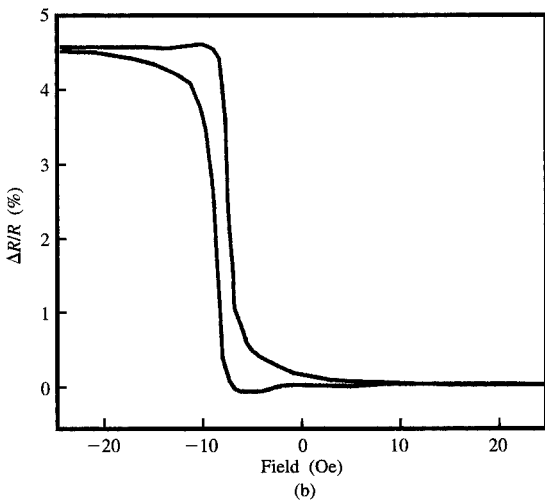
Spin-valve performance was evaluated by fabricating a GMR read head which incorporated the structural elements of its shields for linear resolution, longitudinal bias for stabilization, and lithography for track-width definition. The fabrication of GMR heads is roughly the same as that of AMR heads [27, 28]; both are thin-film sensors with similar operating requirements, differing only in the details of the sensor layers. A GMR head structure is illustrated in **Figure 6**, where P1 designates the lower write pole-tip, P2 designates the upper write pole-tip, $W_{\rm P}$ designates the width of the upper right pole-tip, and $W_{\rm MR}$ designates the track width of the GMR sensor.

• Spin-valve sensor configuration

Using the 1-Gb/in.² spin-valve read head described in [15] as an example, we now discuss the design, fabrication, and

performance of a typical GMR recording head. The head was fabricated using dc magnetron sputter-deposited spin-valve films with a 50 Å Ta/100 Å NiFe/25 Å Cu/22 Å Co/110 Å FeMn structure. The magnetic and spin-valve responses of the free layer along its easy axis are characterized by the low-field measurements shown respectively in **Figure 7**, parts (a) and (b). Both responses exhibit hysteresis loops shifted from zero field. The shift corresponds to a moderate ferromagnetic interlayer coupling field of 8 Oe, equivalent to a coupling energy of 5×10^{-3} ergs/cm². Figure 7(b) also shows the spin-valve coefficient to be ~4.6% and the easy-axis coercivity to be ~1 Oe. Other measurements show the uniaxial anisotropy of the free layer to be 3 Oe, the sheet resistivity of the





Figure

Low-field BH loop (a) and spin-valve response (b) of the NiFe/Cu/FeMn spin-valve sensor.



Figure 8

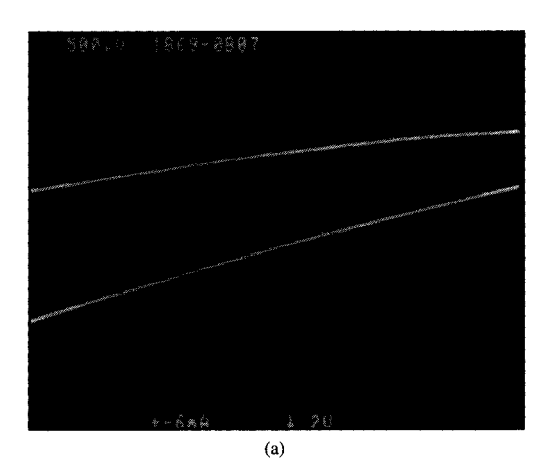
SEM micrograph of spin-valve read head air-bearing surface after lapping.

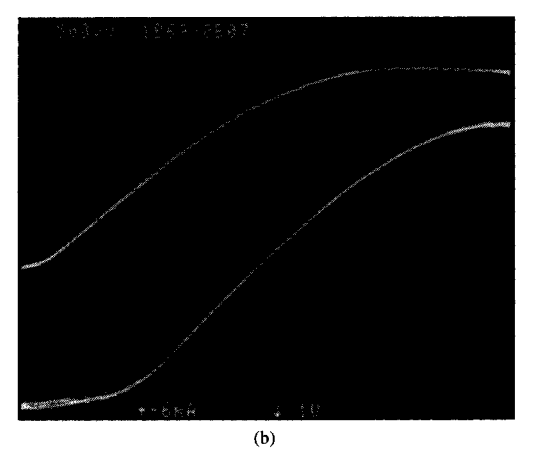
entire structure to be 15.5 Ω/\Box , and the exchange-bias field of the Co/FeMn pinned layer to be as high as 400 Oe.

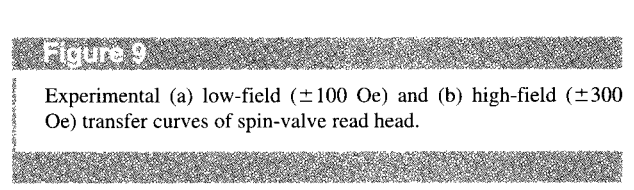
To optimize the linear operating region of the NiFe/Cu/Co spin-valve sensor, the thicknesses of the free and the pinned layers were determined by a micromagnetic modeling study of the sensor behavior in a shielded read head environment, as described earlier. Application of this modeling study to the spin-valve system yielded an optimum thickness combination of 100 Å for the NiFe free layer and 22 Å for the Co pinned layer. Figure 4(a) shows the magnetic bias profile of the free layer, and Figure 4(b) shows the theoretical transfer curve of the optimized design. As discussed in more detail in an earlier section, the quiescent state of the sensor at a 6-mA sense current is close to the center of the linear operating region, resulting in a maximum dynamic range for signal detection.

• Read head fabrication

The optimized spin-valve sensor, with characteristics described above, was incorporated into a shielded read head configuration similar to the gigabit recording head reported previously [2]. The sensor had a nominal read track width of 2 μ m, and was stabilized by longitudinal bias fields applied from the tail regions. The total read gap was 0.25 μ m, with alumina as the gap material and 3- μ m-thick electroplated permalloy layers as the shield material. The material deposition, lithography, and patterning sequence for the spin-valve read head were similar to those employed for a standard MR read head.



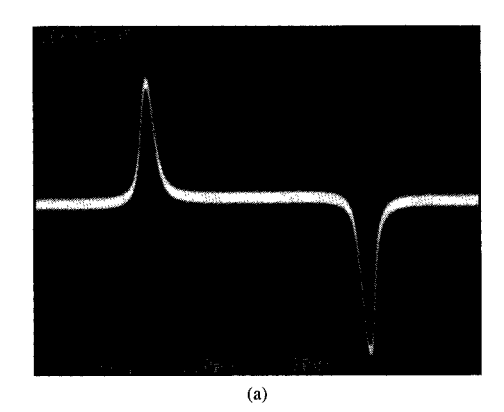




Thermal cycles in the fabrication process were found to result in a sizable reduction in the spin-valve coefficient, yielding a final spin-valve coefficient of only $\sim 3.5\%$ for the spin-valve read heads. After wafer fabrication, the read heads were mechanically lapped to a sensor stripe height of $\sim 1~\mu m$. Figure 8 shows an SEM micrograph of the air-bearing surface of one of the read heads after lapping to final stripe height.

• Transfer curve performance

After slider fabrication and suspension, the heads were studied for their transfer curve behavior under external transverse magnetic field excitation. Figure 9 parts (a) and (b) show the low-field (± 100 Oe) and high-field (± 350 Oe) transfer curves of a 2- μ m-track-width spin-valve head at ± 6 mA sense current, which corresponds to a temperature increase of $\sim 25^{\circ}$ C above ambient. The



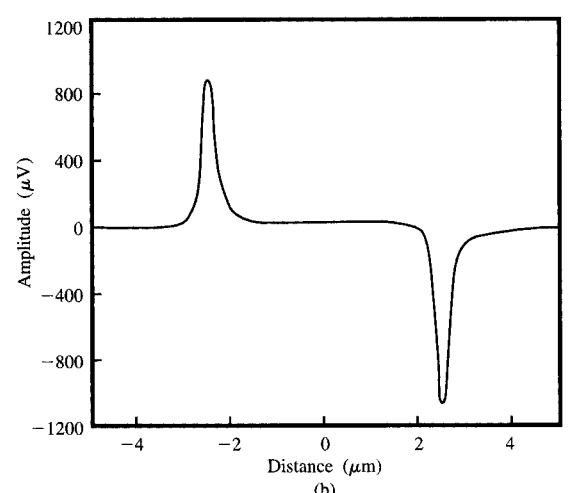


Figure 10

(a) Real-time and (b) averaged read-back waveform of spin-valve head on CoPtCr disk.

transfer curves for the two opposite sense-current polarities were indeed observed to be quite different, reflecting the different quiescent bias states, as illustrated in Figure 4(a). For these spin-valve sensors, the positive current is the design-current direction. This is illustrated by the fact that one sense-current polarity (bottom curves of Figure 9) yielded a large small-signal response amplitude [Figure 9(a)] and a quiescent state fairly close to the middle of the linear operating region [Figure 9(b)]. In contrast, the opposite sense-current polarity yielded a low small-signal response amplitude, and a quiescent bias state closer to magnetic saturation. Next, the high-field transfer curves show a mild convexity in the linear operating region around zero field. This feature was somewhat unexpected from the linearity of the basic GMR behavior, and further analysis showed that it is probably caused by either residual AMR contributions or a small

canting of the pinned layer's magnetic moment from the transverse direction. Figure 9 also shows the GMR response of these narrow-track spin-valve sensors to be quiet, stable, and nonhysteretic for field excitations (±300 Oe) strong enough to induce sensor saturation at the air-bearing surface. This result indicates that the application of a longitudinal bias field from the tail regions is as effective in inducing quiet and single-domain behavior in the spin-valve sensors as in the case of the conventional MR sensors.

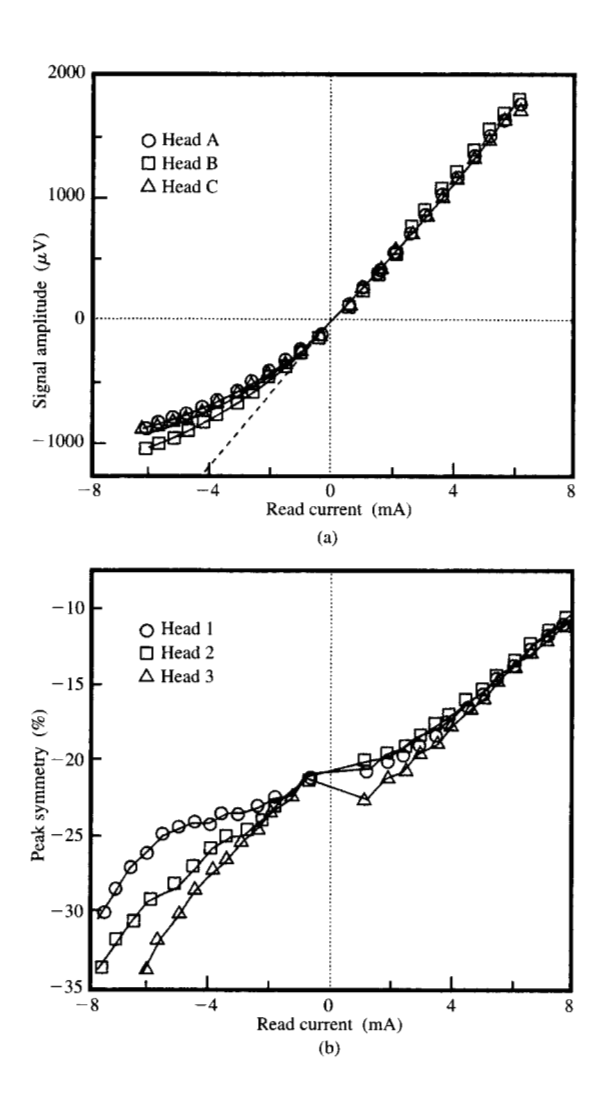
• Recording performance

The recording performance of these spin-valve read heads was tested on CoPtCr thin-film disks with an areal moment as high as 1.25 memu/cm², coercivity of 2500 Oe, and coercive squareness of 0.8. The read heads were operated at currents corresponding to $\sim\!25^{\circ}\mathrm{C}$ temperature increase above ambient, and they were flown at a clearance of $\sim\!1.5~\mu\mathrm{in.}$, corresponding to a total head-disk magnetic spacing of $\sim\!3.0~\mu\mathrm{in.}$ A separate write head was used for data writing. It had a relatively wide write track width of $\sim\!5~\mu\mathrm{m}$ to minimize read-write head misalignment effects.

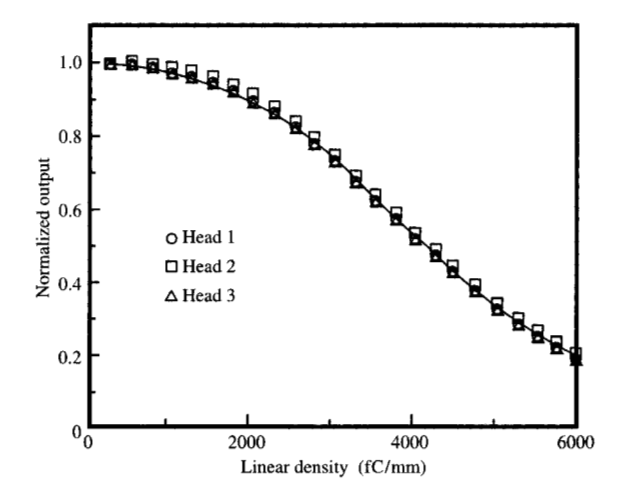
Very large track-width-normalized read-back sensitivities of 750 μ V/ μ m to 1000 μ V/ μ m (peak-to-peak) were observed for these spin-valve heads. This sensitivity range was about a factor of 3 larger than that obtained in our previous gigabit experiment with conventional MR heads [2]. Figure 10 parts (a) and (b) show, respectively, the real-time waveform and the averaged read-back waveform for a 2- μ m-track-width spin-valve sensor. A peak-to-peak signal of $\sim 2000 \,\mu\text{V}$ was achieved, with excellent signal-to-noise conditions free of magnetic instability or noise [Figure 10(a)]. Figure 10(b) shows that both the positive and the negative signal responses exhibit sharp peaks and similar half-widths (PW50), revealing no sign of magnetic saturation despite the high areal moment of the recording media. However, the negative peak is larger than the positive one, yielding a mild amplitude asymmetry of $\sim 10\%$. This amplitude asymmetry might be attributed to the slight transfer curve convexity, as discussed earlier. Next, the variation of the spin-valve head read-back performance with sense current was studied by measuring the signal amplitude [Figure 11(a)] and asymmetry [Figure 11(b)] as a function of the sense current. Figure 11(a) shows the signal amplitude to be roughly linear with sense current along one current direction, but highly sublinear along the other current direction because of the movement of the quiescent bias state from the center of the linear operating region [Figure 3(b)] toward magnetic saturation. This behavior is revealed even more clearly in Figure 11(b), where the amplitude asymmetries decrease rapidly and monotonically as the sense current varies from one direction to its

opposite. These results agree with expectations from our micromagnetic modeling study, highlighting the importance of operating the spin-valve sensor along the correct sense-current direction.

Next, the linear and track density resolutions were studied. Figure 12 shows the linear density roll-off behavior of three spin-valve heads. The signal amplitude decreases monotonically with linear density in a manner typical of the conventional MR sensors as well. To analyze the roll-off data, the transition width was estimated by the



Read-back signal amplitude (a) and peak asymmetry (b) of spinvalve read heads vs. sensor current (amplitude for negative current plotted as negative for clarity; asymmetry defined as difference over sum of the positive and the negative peaks).



Experimental and theoretical roll-off curves of the spin-valve read heads.

Williams-Comstock model with error-function transition profiles, while the read-back process was modeled by the reciprocity principle. Good agreement was found between experimental and theoretical roll-offs at a total head-disk spacing of 3.1 μ in., which was estimated from the flying conditions in our experiment. This agreement between the experiment and the linear read-back model indicates that the spin-valve heads are not magnetically saturated even on disks with areal moments as high as 1.25 memu/cm². It confirms the large signal range capability for spin-valve sensors, as expected when the magnetic moment of the free layer is along the longitudinal direction. The 50% roll-off densities were around 4200 fC/mm, which are toward the lower end of the roll-off densities measured in the previous gigabit experiment [2]. This was mainly the result of broader transition profiles from a higher areal moment. To improve the linear resolution, therefore, some of the amplitude performance might be traded off by using a medium with a lower areal moment (e.g., ~ 1 memu/cm²). A better approach is to redesign the spin-valve sensor with a thinner free layer so that it fits optimally with a lower-areal-moment medium. Finally, the track resolution was studied by measuring the microtrack profile of the spin-valve heads. In this measurement, the data track was first reduced to $\sim 0.2 \mu m$ in track width by erasure from the sides. The spin-valve head was then scanned over this microtrack while the signal at the fundamental data frequency was recorded. Results (Figure 13) show well-behaving read head profiles obtained with rapidly and monotonically decreasing signal amplitudes

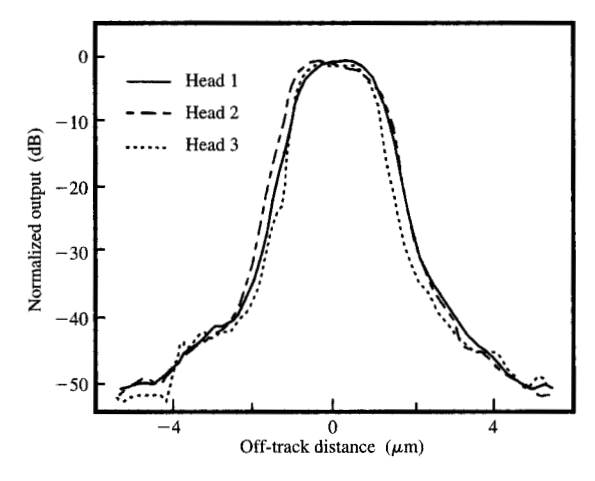


Figure 13

Microtrack profiles of the spin-valve read heads.

as the head was moved off-track. The profiles were also symmetrical between the two opposite off-track directions because of the orientation of the free-layer magnetic moment along the longitudinal "unbiased" direction. This behavior was in distinct contrast to those for the conventional MR heads, which often exhibit pronounced left-right asymmetries as well as compensation-point behaviors [2]. The half widths of the profiles yielded read track widths around 2 μ m, in agreement with the design target. The widths of the profiles at -30 dB were only \sim 4.5 μ m, much smaller than those for the conventional MR sensor in the previous gigabit experiment [2]. This reduction of side reading is a result of several factors, including the thinness of the free layer, the magnetic rigidity of the pinned layer, and the "unbiased" quiescent state of the free layer.

Conclusions

In this paper, we have analyzed the potentials of GMR sensors for very high-data-rate and very high-density magnetic recording. We have also highlighted the multitude of technical issues related to the biasing, stabilization, and fabrication of such sensors. In all, we have shown that the immense promise of the GMR sensors is matched by significant challenges in their materials, processing, and sensor design. However, just as inductive read heads of the present are giving way to MR heads, so MR heads in the future will almost certainly give way to GMR heads in order to satisfy the pressing need for increases in data densities and data rates.

Indeed, judging from the intensity of industry-wide efforts and the rapidity of progress in GMR head design, materials, and processes, this second transition is expected to be forthcoming in the near future.

*Trademark or registered trademark of International Business Machines Corporation.

References

- R. Hunt, "A Magnetoresistive Readout Transducer," IEEE Trans. Magn. MAG-7, No. 1, 150-154 (1971).
- C. Tsang, M. Chen, T. Yogi, and K. Ju, "Gigabit Density Recording Using Dual-Element MR/Inductive Heads on Thin-Film Disks," *IEEE Trans. Magn.* 26, No. 5, 1689–1693 (1990).
- C. Tsang, "Design and Performance Considerations in High Areal Density Longitudinal Magnetic Recording," J. Appl. Phys. 69, No. 8, 5393-5398 (1991).
- C. Tsang, H. Santini, D. McCown, J. Lo, and R. Lee, "3 Gb/in² Recording Demonstration with Dual Element Heads and Thin Film Disks," *IEEE Trans. Magn.* 32, No. 1, 7–12 (1996).
- C. Tsang, T. Lin, S. MacDonald, N. Robertson, H. Santini, M. Doerner, T. Reith, L. Vo, T. Diola, and P. Arnett, "5 Gb/in² Recording Demonstration with Conventional AMR Dual Element Heads and Thin Film Disks," *IEEE Trans. Magn.* 33, No. 5, 2866–2871 (1997).
- M. Baibich, J. Broto, A. Fert, F. Nguyen Van Dau, and F. Petroff, "Giant Magnetoresistance of (001)Fe/(001)Cr Magnetic Superlattices," *Phys. Rev. Lett.* 61, No. 21, 2472–2475 (1988).
- B. Dieny, V. Speriosu, S. Parkin, P. Baumgart, and D. Wilhoit, "Magnetotransport Properties of Magnetically Soft Spin-Valve Structure," *J. Appl. Phys.* 69, No. 8, 4774-4779 (1991).
- S. Parkin, "Dramatic Enhancement of Interlayer Exchange Coupling and Giant Magnetoresistance in Ni₈₁Fe₁₉/Cu by Addition of Thin Co Interface Layers," *Appl. Phys. Lett.* 61, No. 11, 1358–1360 (1991).
- 9. R. White, "Giant Magnetoresistance: A Primer," *IEEE Trans. Magn.* 28, No. 5, 2482–2487 (1992).
- J. Daughton, P. Bade, M. Jenson, and M. Rahmati, "Giant Magnetoresistance in Narrow Stripes," *IEEE Trans. Magn.* 28, No. 5, 2488–2493 (1992).
- A. Berkowitz, J. Mitchell, M. Corey, and A. Young, "Giant Magnetoresistance in Heterogeneous Cu-Co Alloys," *Phys. Rev. Lett.* 68, No. 25, 3745–3748 (1992).
- T. Hylton, K. Coffey, M. Parker, and J. Howard, "Giant Magnetoresistance at Low Fields in Discontinuous NiFe-Ag Multilayer Thin Films," *Science* 261, 1021-1024 (1992).
- T. Huang, J. Nozieres, V. Speriosu, B. Gurney, and H. Lefakis, "Effect of Annealing on the Interfaces of Giant-Magnetoresistance Spin-Valve Structure," *Appl. Phys. Lett.* 62, No. 13, 1478–1480 (1993).
- D. Heim, R. Fontana, C. Tsang, V. Speriosu, B. Gurney, and M. Williams, "Design and Operation of Spin Valve Sensors," *IEEE Trans. Magn.* 30, No. 2, 316–321 (1994).
- C. Tsang, R. Fontana, T. Lin, D. Heim, V. Speriosu, B. Gurney, and M. Williams, "Design, Fabrication and Testing of Spin-Valve Read Heads for High Density Recording," *IEEE Trans. Magn.* 30, 3801–3806 (1994).
- M. Parker, K. Coffrey, J. Howard, C. Tsang, R. Fontana, and T. Hylton, "Overview of Progress in Giant Magnetoresistive Sensors Based on NiFe/Ag Multilayers," *IEEE Trans. Magn.* 32, No. 1, 142–148 (1996).
- Y. Hamakawa, H. Hoshiya, T. Kawabe, Y. Suzuki, R. Arai, K. Nakamoto, M. Fuyama, and Y. Sugita, "Spin-

- Valve Heads Utilizing Antiferromagnetic NiO Layers," *IEEE Trans. Magn.* **32**, No. 1, 149–155 (1996).
- H. Yoda, H. Iwasaki, T. Kobayashi, A. Tsutai, and M. Sahashi, "Dual-Element GMR/Inductive Heads for Gigabits Density Recording Using CoFe Spin-Valves," *IEEE Trans. Magn.* 32, No. 5, 3363–3367 (1996).
- H. Kanai, K. Yamada, K. Aoshima, Y. Ohtsuka, J. Kane, M. Kanamine, J. Toda, and Y. Mizoshita, "Spin-Valve Read Heads with NiFe/Co90Fe10 Layers for 5 Gbit/in² Density Recording," *IEEE Trans. Magn.* 32, No. 5, 3368–3373 (1996).
- K. Nakamoto, Y. Kawato, Y. Suzuki, Y. Hamakawa, T. Kawabe, K. Fujimoto, M. Fuyama, and Y. Sugita, "Design and Read Performance of GMR Heads with NiO," *IEEE Trans. Magn.* 32, No. 5, 3374-3379 (1996).
- S. Decker and C. Tsang, "Magnetoresistive Response of Small Permalloy Features," J. Appl. Phys. 16, No. 5, 643-645 (1980).
- C. Tsang and S. Decker, "The Origin of Barkhausen Noise in Small Permalloy Magnetoresistive Sensors," J. Appl. Phys. 52, No. 3, 2465-2467 (1981).
- C. Tsang, "Magnetics of Small Magnetoresistive Sensors,"
 J. Appl. Phys. 55, 2226-2231 (1981).
- 24. C. Tsang, "Unshielded MR Elements with Patterned Exchange-Biasing," *IEEE Trans. Magn.* 25, No. 5, 3692–3694 (1989).
- T. Lin, C. Tsang, R. Fontana, and J. Howard, "Exchange-Coupled NiFe/FeMn, NiFe/NiMn and NiO/NiFe Films for Stabilization of Magnetoresistive Sensors," *IEEE Trans. Magn.* 31, No. 6, 2585–2590 (1995).
- T. Lin, G. Gorman, and C. Tsang, "Antiferromagnetic and Hard Magnetic Stabilization Schemes for Magnetoresistive Sensors," *IEEE Trans. Magn.* 32, No. 5, 3443-3445 (1996).
- 27. R. Fontana, "Process Complexity of Magnetoresistive Sensors: A Review," *IEEE Trans. Magn.* 31, No. 6, 2579–2584 (1995).
- R. Fontana, S. MacDonald, C. Tsang, and T. Lin, "Submicron Trackwidth and Stripe Height MR Sensor Test Structures," *IEEE Trans. Magn.* 32, No. 5, 3440–3445 (1996).

Received July 29, 1997; accepted for publication October 22, 1997

Ching H. Tsang IBM Research Division, Almaden Research Center, 650 Harry Road, San Jose, California 95120 (TSANG at ALMVMA, tsang@almaden.ibm.com). Dr. Tsang is an IBM Fellow. He received his B.S. degree in electrical engineering from Case Western Reserve University, and his M.S. and Ph.D. degrees from Stanford University. From 1977 to 1978 he worked at the Xerox Palo Alto Research Center on the optical and electrical properties of amorphous semiconductors. Since 1978 he has been with IBM Research in San Jose, California, working on the physics, design, and performance of magnetoresistive recording heads. He has also worked on the physics and applications of magnetic multilayer films, as well as numerous topics in recording physics, including various types of nonlinear transition shifts. Dr. Tsang's current interests include very high-density magnetic recording and the application of giant magnetoresistance sensors to magnetic recording. He has more than 40 publications and is a Fellow of the Institute of Electrical and Electronics Engineers.

Robert E. Fontana, Jr. IBM Research Division, Almaden Research Center, 650 Harry Road, San Jose, California 95120 (FONTANA at ALMVMA, fontana@almaden.ibm.com). Dr. Fontana is a Research Staff Member in the Storage Systems and Technology Department at the IBM Almaden Research Center with responsibility for thin-film processing of advanced magnetic recording transducers. He received B.S., M.S., and Ph.D. degrees in electrical engineering from the Massachusetts Institute of Technology in 1969, 1971, and 1975, respectively. From 1975 to 1981 he worked at Texas Instruments, Inc., developing thin-film processing techniques for magnetic bubble memory devices. In 1981 Dr. Fontana joined the IBM Research Division in San Jose, California, working on processing issues related to thin-film magnetoresistive heads. He has received three IBM Outstanding Technical Achievement Awards and an IBM Corporate Award for his work in magnetoresistive thin-film head processing. Dr. Fontana is a Fellow of the Institute of Electrical and Electronics Engineers.

Tsann Lin IBM Storage Systems Division, 5600 Cottle Road. San Jose, California 95193 (tsann@almaden.ibm.com) Dr. Lin is a Senior Engineer/Scientist in the Advanced Film Head Processing Department at the IBM Almaden Research Center. He received B.S. and M.S. degrees in materials science and engineering from the National Tsin Hua University, Taiwan, Republic of China, in 1977 and 1979, respectively, and a Ph.D. degree in materials science and engineering from the University of California at Berkeley in 1986. Dr. Lin subsequently joined IBM at the Thomas J. Watson Research Center, where he has worked on thin-film metallurgy and interconnections in integrated circuit devices. In 1989 he joined the IBM Storage Systems Division, where he has been working on the fabrication processes of AMR and GMR heads used for post-gigabit densities, and on exploration of thin-film materials used for AMR and GMR sensors, antiferromagnetic and hard-magnetic stabilization of the sensors, conductor leads, and high-magnetization write poles. Dr. Lin is a member of the IEEE Magnetics Society and the Magnetics Society of Japan.

David E. Heim IBM Storage Systems Division, 5600 Cottle Road, San Jose, California 95193 (deheim@vnet.ibm.com). Dr. Heim received his Ph.D. degree from the University of California at San Diego in 1981 in theoretical condensedmatter physics. He subsequently joined the IBM Storage

Systems Division, where he has been employed in modeling the performance and behavior of thin-film recording heads (inductive read/write, AMR, and GMR-SV). Dr. Heim is a member of the IEEE Magnetics Society.

Bruce A. Gurney IBM Research Division, Almaden Research Center, 650 Harry Road, San Jose, California 95120 (GURNEY at ALMADEN, gurney@almaden.ibm.com). Dr. Gurney is a Research Staff Member at the IBM Almaden Research Center, where he has been investigating the fundamental underpinnings of present and future magnetic recording technologies since 1987. For much of that time he has investigated the mechanisms of magnetotransport in giant magnetoresistance and spin-valve layered materials. His work emphasizes the application of these materials to read-back sensors; in this field he has authored more than a dozen papers, and he holds fourteen patents. He received a B.S. degree (1979) in physics from the California Institute of Technology, followed by M.S. (1982) and Ph.D. (1987) degrees in physics from Cornell University, where he developed novel instrumentation for the investigation of physical and chemical processes at surfaces. In 1992 Dr. Gurney shared in an IBM Outstanding Technical Achievement Award for the development of spin valves. He is a member of the American Physical Society, the American Vacuum Society, the Institute of Electrical and Electronics Engineers, and the Materials Research Society.

Mason L. Williams IBM Research Division, Almaden Research Center, 650 Harry Road, San Jose, California 95120 (WILMSML at ALMADEN, wilmsml@almaden.ibm.com). Dr. Williams is a Research Staff Member in the Recording Heads Department at the IBM Almaden Research Center. He received a B.S. degree in engineering from the California Institute of Technology in 1964, and M.S. and Ph.D. degrees in electrical engineering from the University of Southern California in 1966 and 1970, respectively. He subsequently joined IBM in San Jose, where he has worked on magnetic recording technology. Dr. Williams is a senior member of the Institute of Electrical and Electronics Engineers.